High-Order Similarity Relations in Radiative Transfer: Supplementary Document

Shuang Zhao
Cornell University

Ravi Ramamoorthi
University of California, Berkeley

Kavita Bala
Cornell University

Overview

This is the supplementary document for our SIGGRAPH 2014 paper titled "High-Order Similarity Relations in Radiative Transfer".

- Section 1 describes the similarity relations described in Section 4.1 of the paper.
- Section 2 shows the connection between similarity theory and classical diffusion theory. We present an alternative derivation of the diffusion equation (DE) based on the assumption that the radiance field is *linearly anisotropic*, which is shared by the order-1 similarity relation.
- Based on Section 2, we show in Section 3 a generalization of the order-1 similarity relation, following the derivation introduced by Wyman et al. [1989b].
- Section 4 provides background on a function's *monomial* and *Legendre moments*.

The rest of this document shows extra results.

- Section 5 contains the rendered images used to create the plots in Figure 6 of the paper. This figure discusses how the user-specified parameter α affects performance and accuracy.
- Section 6 provides two examples of overfitting. This issue has been discussed in Section 7.3 of the paper.
- Section 7 shows the rendered images and the corresponding phase functions used to create the three 2D embeddings in Figure 9 of the paper. These results demonstrate that to accurately capture important visual cues, higher-order analysis is crucial.

1 Recap: Similarity Relations

For completeness of this document, this section restates the similarity relations introduced by Wyman et al. [1989a] and presented in Section 4.1 of the paper.

We are given a radiative transfer equation (RTE)[1]

$$(\boldsymbol{\omega}\cdot\nabla)L(\boldsymbol{\omega}) = -\sigma_t L(\boldsymbol{\omega}) + \sigma_s \int_{\mathbb{S}^2} f(\boldsymbol{\omega}'\cdot\boldsymbol{\omega})L(\boldsymbol{\omega}')\,\mathrm{d}\boldsymbol{\omega}' \tag{1}$$

and an altered version

$$(\boldsymbol{\omega}\cdot\nabla)L(\boldsymbol{\omega}) = -\sigma_t^* L(\boldsymbol{\omega}) + \sigma_s^* \int_{\mathbb{S}^2} f^*(\boldsymbol{\omega}'\cdot\boldsymbol{\omega})L(\boldsymbol{\omega}')\,\mathrm{d}\boldsymbol{\omega}' \tag{2}$$

with identical boundary conditions. Assume that the solution radiance field L of (1) has limited angular frequency, namely

$$a_{mn} = 0 \quad \text{for} \quad n > N,\ -n \le m \le n \tag{3}$$

for some fixed N. Then (2) has the same solution L as (1) if the ***similarity relation of order*** N:

$$\begin{aligned} \sigma_a &= \sigma_a^*, \\ \sigma_s(1-f_n) &= \sigma_s^*(1-f_n^*) \quad \text{for} \quad 1 \le n \le N \end{aligned} \tag{4}$$

[1] We assume that the medium has no internal source, so Q vanishes.

holds where f_n, f_n^* denote the n-th Legendre moments of phase functions $f(\cdot)$, $f^*(\cdot)$, respectively. See Section 4 for more information on function moments.

2 Derivation of the Diffusion Equation

In this section, we present an alternative derivation of the diffusion equation (DE) based on the same assumption taken by the order-1 similarity relation: the radiance field L is *linearly anisotropic*, namely

$$a_{mn} = 0 \quad \text{for all} \quad n > 1. \tag{5}$$

We first rewrite the RTE (1) in a series of integrated forms (Section 2.1). Then, we present in Section 2.2 the order-0 and order-1 versions of the integrated RTE and simplify them based on the assumption (5). Finally, we combine the results from Section 2.2 to obtain the DE (Section 2.3).

A similar derivation has been proposed by Wyman et al. [1989b] to obtain the generalized similarity relations described in Section 3.

2.1 Integrated RTE

Let

$$\omega_{i_1 i_2 \dots i_n} := \prod_{j=1}^{n} \omega_{i_j}$$

where ω_{i_j} denotes the i_j-th component of $\boldsymbol{\omega}$, which is a 3-vector (so $i_j \in \{1,2,3\}$ for all j). In addition, we define the integrated forms of the three terms (including the source term Q) appearing in the RHS of the RTE (1):

$$\phi_{i_1 i_2 \dots i_n} := \int_{\mathbb{S}^2} \omega_{i_1 i_2 \dots i_n} L(\boldsymbol{\omega})\,\mathrm{d}\boldsymbol{\omega}, \tag{6}$$

$$\chi_{i_1 i_2 \dots i_n} := \int_{\mathbb{S}^2}\int_{\mathbb{S}^2} \omega_{i_1 i_2 \dots i_n} f(\boldsymbol{\omega}'\cdot\boldsymbol{\omega})L(\boldsymbol{\omega}')\,\mathrm{d}\boldsymbol{\omega}'\,\mathrm{d}\boldsymbol{\omega}, \tag{7}$$

$$Q_{i_1 i_2 \dots i_n} := \int_{\mathbb{S}^2} \omega_{i_1 i_2 \dots i_n} Q(\boldsymbol{\omega})\,\mathrm{d}\boldsymbol{\omega}. \tag{8}$$

An integrated version of the RTE (1) can then be obtained by multiplying $\omega_{i_1 i_2 \dots i_n}$ and integrating over $\mathbb{S}^2$ on both sides, yielding

$$\sum_{j=1}^{3} \partial_j \phi_{j i_1 \dots i_n} = -\sigma_t \phi_{i_1 \dots i_n} + \sigma_s \chi_{i_1 \dots i_n} + Q_{i_1 \dots i_n} \tag{9}$$

where ∂_i denotes $\frac{\partial}{\partial \omega_i}$.

2.2 Order-0 and Order-1 Versions

We now write down the order-0 and order-1 versions of the integrated RTE (9) and simplify them based on (5).

Order-0. The order-0 version of (9) is

$$\sum_{j=1}^{3} \partial_j \phi_j = -\sigma_t \phi + \sigma_s \chi + Q_{(0)} \tag{10}$$

where $Q_{(0)} := \int_{\mathbb{S}^2} Q(\boldsymbol{\omega})\,\mathrm{d}\boldsymbol{\omega}$. Since

$$\chi = \int_{\mathbb{S}^2} L(\boldsymbol{\omega}') \int_{\mathbb{S}^2} f(\boldsymbol{\omega}' \cdot \boldsymbol{\omega})\,\mathrm{d}\boldsymbol{\omega}\,\mathrm{d}\boldsymbol{\omega}' = \int_{\mathbb{S}^2} L(\boldsymbol{\omega}')\,\mathrm{d}\boldsymbol{\omega}' = \phi,$$

(10) simplifies to

$$\sum_{j=1}^{3} \partial_j \phi_j = -\sigma_a \phi + Q_{(0)}. \tag{11}$$

Order-1. The order-1 version of (9) is

$$\sum_{j=1}^{3} \partial_j \phi_{ji} = -\sigma_t \phi_i + \sigma_s \chi_i + Q_i. \tag{12}$$

Due to (5), it holds that

$$\begin{aligned}
\chi_i &= \int_{\mathbb{S}^2} \int_{\mathbb{S}^2} \omega_i f(\boldsymbol{\omega}' \cdot \boldsymbol{\omega}) L(\boldsymbol{\omega}')\,\mathrm{d}\boldsymbol{\omega}'\,\mathrm{d}\boldsymbol{\omega} \\
&= \sum_{n=0}^{\infty} \sum_{m=-n}^{n} \sum_{i=0}^{1} \sum_{j=-i}^{i} f_n a_{ji} \\
&\quad \left(\int_{\mathbb{S}^2} \omega_i Y_n^m(\boldsymbol{\omega}) \underbrace{\int_{\mathbb{S}^2} \bar{Y}_n^m(\boldsymbol{\omega}') Y_i^j(\boldsymbol{\omega}')\,\mathrm{d}\boldsymbol{\omega}'}_{=\,\delta_{ni}\ \delta_{mj}}\,\mathrm{d}\boldsymbol{\omega} \right) \\
&= \sum_{n=0}^{1} \sum_{m=-n}^{n} f_n a_{mn} \int_{\mathbb{S}^2} \omega_i Y_n^m(\boldsymbol{\omega})\,\mathrm{d}\boldsymbol{\omega} \\
&= f_1 \sum_{m=-1}^{1} a_{m1} \int_{\mathbb{S}^2} \omega_i Y_1^m(\boldsymbol{\omega})\,\mathrm{d}\boldsymbol{\omega}
\end{aligned} \tag{13}$$

where the last equality follows the fact that $\int_{\mathbb{S}^2} \omega_i Y_0^0(\boldsymbol{\omega})\,\mathrm{d}\boldsymbol{\omega} = 0$ for all $i \in \{1,2,3\}$. Similarly, we have

$$\phi_i = \int_{\mathbb{S}^2} \omega_i L(\boldsymbol{\omega})\,\mathrm{d}\boldsymbol{\omega} = \sum_{m=-1}^{1} a_{m1} \int_{\mathbb{S}^2} \omega_i Y_1^m(\boldsymbol{\omega})\,\mathrm{d}\boldsymbol{\omega}. \tag{14}$$

From (13) and (14), we know that

$$\chi_i = f_1 \phi_i. \tag{15}$$

It is easy to verify that for all i_1 and i_2, $\int_{\mathbb{S}^2} \omega_{i_1 i_2} Y_0^0(\boldsymbol{\omega})\,\mathrm{d}\boldsymbol{\omega} = \frac{2\sqrt{\pi}}{3}\delta_{i_1 i_2}$ and $\int_{\mathbb{S}^2} \omega_{i_1 i_2} Y_1^m(\boldsymbol{\omega})\,\mathrm{d}\boldsymbol{\omega} = 0$. Thus,

$$\phi_{i_1 i_2} = \int_{\mathbb{S}^2} \omega_{i_1 i_2} L(\boldsymbol{\omega})\,\mathrm{d}\boldsymbol{\omega} = a_{00} \frac{2\sqrt{\pi}}{3} \delta_{i_1 i_2}.$$

Note that $a_{00} = \int_{\mathbb{S}^2} Y_0^0(\boldsymbol{\omega}) L(\boldsymbol{\omega})\,\mathrm{d}\boldsymbol{\omega} = \frac{\phi}{2\sqrt{\pi}}$, we have

$$\phi_{i_1 i_2} = \frac{\phi}{3} \delta_{i_1 i_2}. \tag{16}$$

Substituting (15) and (16) into (12) leads to

$$\frac{1}{3} \partial_i \phi = -\sigma_{tr,1} \phi_i + Q_i \tag{17}$$

where $\sigma_{tr,1} = \sigma_t - f_1 \sigma_s$ follows the definition in (11) of the paper.

2.3 Diffusion Equation

In this subsection, we show that the DE can be obtained easily from the integrated RTE (9) in its simplified order-0 (11) and order-1 (17) forms.

Let

$$\mathbf{E} := \int_{\mathbb{S}^2} \boldsymbol{\omega} L(\boldsymbol{\omega})\,\mathrm{d}\boldsymbol{\omega} = \begin{pmatrix} \phi_1 \\ \phi_2 \\ \phi_3 \end{pmatrix}, \quad \mathbf{Q}_{(1)} := \begin{pmatrix} Q_1 \\ Q_2 \\ Q_3 \end{pmatrix},$$

and $\kappa := (3\sigma_{tr,1})^{-1}$. Then (11) and (17) can be rewritten as

$$\nabla \cdot \mathbf{E} = -\sigma_a \phi + Q_{(0)}, \tag{18}$$

$$\mathbf{E} = 3\kappa \mathbf{Q}_{(1)} - \kappa \nabla \phi \tag{19}$$

where $\nabla\cdot$ is the divergence operator and ∇ is the gradient operator. Substituting (19) into (18) yields

$$\nabla \cdot \left(3\kappa \mathbf{Q}_{(1)} - \kappa \nabla \phi\right) = 3\kappa\, \nabla \cdot \mathbf{Q}_{(1)} - \nabla \cdot (\kappa \nabla \phi) = -\sigma_a \phi + Q_{(0)}.$$

Namely,

$$-\nabla \cdot (\kappa \nabla \phi) + \sigma_a \phi = Q_{(0)} - 3\kappa\, \nabla \cdot \mathbf{Q}_{(1)}, \tag{20}$$

and (20) is known as the *diffusion equation*.

3 Generalized Order-1 Similarity Relation

The similarity relations (4) requires $\sigma_a^* = \sigma_a$ to ensure that the altered RTE (2) has the same solution radiance field L as the original (1). However, if we relax this equal-radiance constraint and only ask for the same *fluence* $\phi = \int_{\mathbb{S}^2} L(\boldsymbol{\omega})\,\mathrm{d}\boldsymbol{\omega}$, generalized versions of the similarity relations can be derived [Wyman et al. 1989b]. Unlike (4), unfortunately, these relations do not easily generalize to higher orders.

Assuming (5) holds, namely the radiance field is linearly anisotropic, (11) and (17) can be used to derive the generalized similarity relation of order-1 as follows. Applying ∂_i and summing over 1 to 3 on both sides of (17) and substituting (11) into the resulting equation yields

$$\sum_{i=1}^{3} \partial_i^2 \phi = \sigma_a \sigma_{tr,1} \phi - \sigma_{tr,1} Q_{(0)} + \sum_{i=1}^{3} \partial_i Q_i.$$

For participating media with no internal source, all moments of Q vanish, giving $\sigma_a \sigma_{tr,1} \phi - \sum_i \partial_i^2 \phi = 0$. Similarly, it holds that $\sigma_a^* \sigma_{tr,1}^* \phi - \sum_i \partial_i^2 \phi = 0$. Equating these two equations yields

$$\sigma_a \sigma_{tr,1} = \sigma_a^* \sigma_{tr,1}^*, \tag{21}$$

which is the order-1 generalized similarity relation. In addition, it has been shown in [Wyman et al. 1989b] that the solution radiance field L of the original RTE and the solution L^* of the altered one are related as follows:

$$L(\boldsymbol{\omega}) = \frac{\sigma_a}{\sigma_a^*} L^*(\boldsymbol{\omega}) + \left(1 - \frac{\sigma_a}{\sigma_a^*}\right) \frac{\phi}{4\pi}. \tag{22}$$

Note that when $\sigma_a^* = \sigma_a$, (22) collapses to $L(\boldsymbol{\omega}) = L^*(\boldsymbol{\omega})$ and (21) becomes the order-1 similarity relation, namely (4) with $N = 1$.

4 Phase Function Moments

Given a phase function $f(\cdot)$, its *monomial moments* and *Legendre moments* are defined as follows.

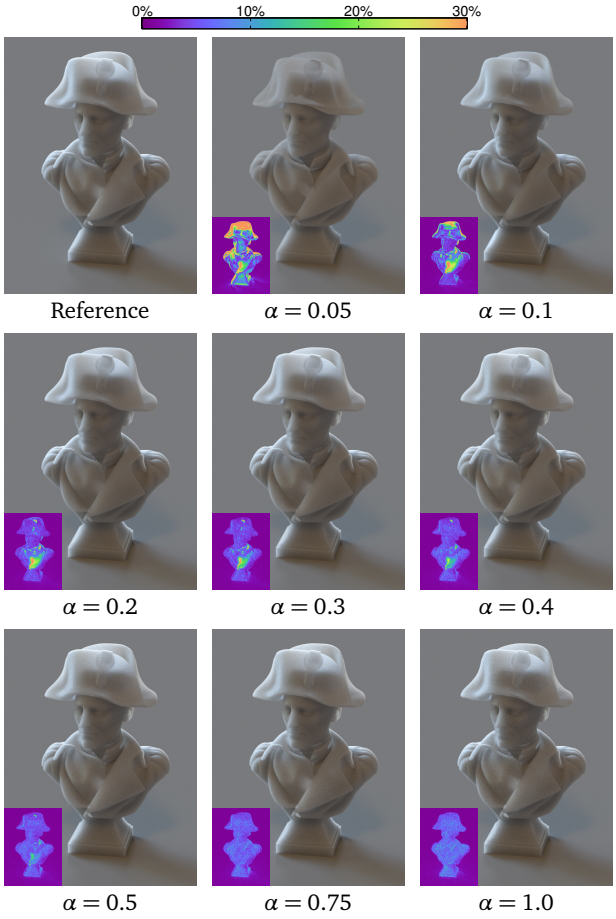

Figure 1: *Rendered images used to create the orange curve in Figure 6 of the paper. The relative error maps (using the color mapping shown at the top) are included.*

Monomial Moments. Given $f(\cdot)$, its n-th monomial moment is

$$\gamma_n := \int_{-1}^{1} f(t)\, t^n \, \mathrm{d}t. \tag{23}$$

Legendre Moments. Given $f(\cdot)$, its n-th Legendre moment is

$$f_n := 2\pi \int_{-1}^{1} f(t) P_n(t) \, \mathrm{d}t \tag{24}$$

where P_n denotes the degree-n Legendre polynomial and 2π is a normalization term. Since $f(\cdot)$ is a phase function, it holds that

$$f_0 = 2\pi \int_{-1}^{1} f(t)\, \mathrm{d}t = \int_{\mathbb{S}^2} f(\cos\theta)\, \mathrm{d}\boldsymbol{\omega} \equiv 1 \tag{25}$$

and

$$f_1 = 2\pi \int_{-1}^{1} t f(t)\, \mathrm{d}t = \int_{\mathbb{S}^2} \cos\theta f(\cos\theta)\, \mathrm{d}\boldsymbol{\omega} \tag{26}$$

where θ is the angle between $\boldsymbol{\omega}$ and the incident direction. f_1 is usually referred to as the *average cosine* of $f(\cdot)$. For a Henyey-Greenstein (HG) phase function with parameter g, its n-th Legendre moment has been shown to equal g^n (see Theorem 7.1 in [Van den Eynde 2005]).

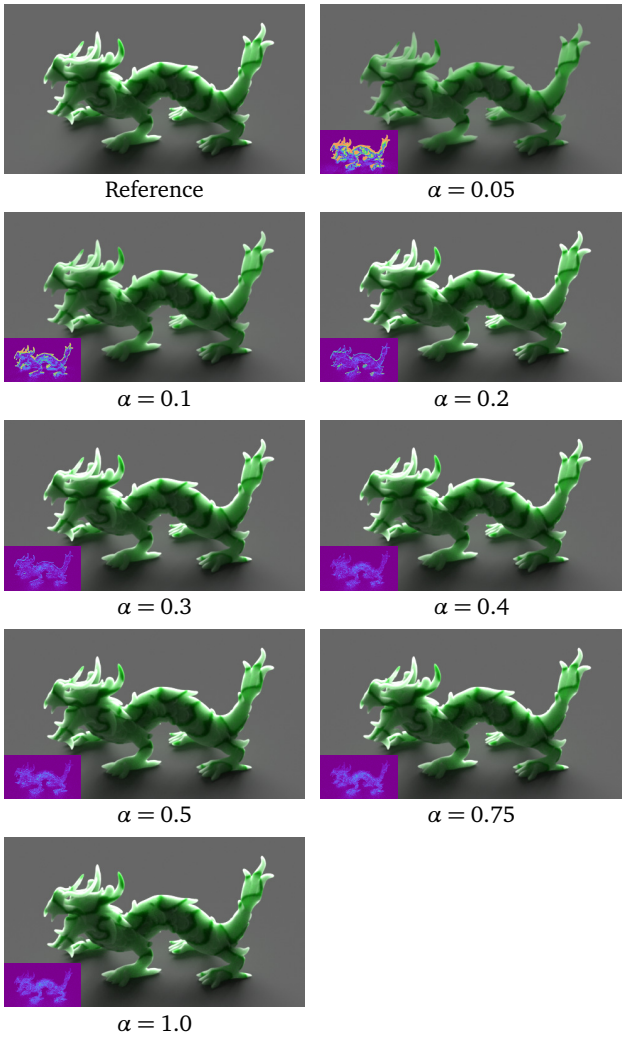

Figure 2: *Rendered images corresponding to the purple curve in Figure 6 of the paper. The relative error visualizations use the same color mapping as Figure 1.*

In fact, monomial moments and Legendre moments are closely related. Precisely, for any $N \geq 0$, the first $(N+1)$ Legendre moments and the first $(N+1)$ monomial moments *uniquely determine* each other. In other words, any phase function $f(\cdot)$ with $f_0, \ldots, f_N$ fixed will have the same $\gamma_0, \ldots, \gamma_N$, and vice versa.

Proof. Let $P_n(t) = \sum_{i=0}^{n} p_{n,i}\, t^i$. According to (23) and (24), we know that for any $n \geq 0$,

$$f_n = 2\pi \sum_{i=0}^{n} \Big(p_{n,i} \underbrace{\int_{-1}^{1} f(t)\, t^i \, \mathrm{d}t}_{=\gamma_i} \Big). \tag{27}$$

Let $\boldsymbol{\gamma} := (\gamma_0\ \gamma_1\ \ldots\ \gamma_N)^T$ and $\mathbf{f} := (f_0\ f_1\ \ldots\ f_N)^T$, equation (27) can be rewritten in vector form as

$$\mathbf{f} = 2\pi \hat{\mathbf{P}} \boldsymbol{\gamma}. \tag{28}$$

where $\hat{\mathbf{P}}$ is an $(N+1) \times (N+1)$ matrix with $\hat{P}(i+1, j+1) = p_{i,j}$ for $0 \leq i, j \leq N$. It is easy to verify that $\hat{\mathbf{P}}$ is lower-triangular and non-singular. Thus, $\boldsymbol{\gamma}$ and $\mathbf{f}$ uniquely determine each other. Given $\mathbf{f}$, $\boldsymbol{\gamma}$ can be computed by solving the linear system in (28). ∎

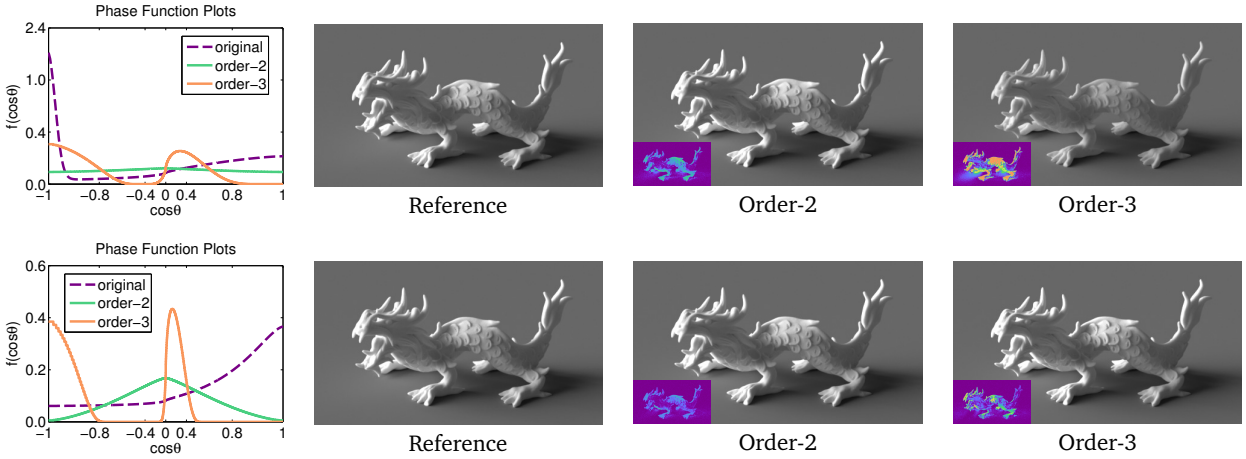

Figure 3: *Two examples on overfitting. In both examples, the altered parameters satisfying the order-3 similarity relation overfit.*

5 Results: Performance versus Accuracy

Figures 1 and 2 contain rendered images we used to study how α, the user-specified parameter, controls the balance between performance and accuracy.

5.1 Bust

The renderings in Figure 1 correspond to the orange curve in Figure 6 of the paper. The environment lighting used in the following rendering is "Kitchen" from [Debevec 1998]. Note that

- The $\alpha = 1$ result is not identical to the reference since the latter was rendered with a much higher number of samples.
- The error in the results with high α values are mostly from Monte Carlo noise.

5.2 Dragon

The renderings in Figure 2 correspond to the purple curve in Figure 6 of the paper. We used the environment lighting "Ennis" from [Debevec 1998]. Similar to Figure 1, the reference image was rendered using a higher number of sample paths per pixel.

6 Results: Overfitting

In our experiments, overfitting does not happen very often and normally causes only subtle differences. Figure 3 illustrates two examples where altered parameters adhering to the order-3 similarity relation overfit. Our method (Algorithm 1 in the paper) successfully rejects these solutions (and returns the order-2 versions) since their coverages are too small (which is demonstrated by the phase functions plots).

7 Results: Spanning the Perceptual Space

This section includes the images we used to create the embeddings in Figure 9 of the paper. The two examples in Figure 9-cde correspond to phase functions 18 and 35.

7.1 Rendered Images

This section illustrates 40 rows of images, and each row corresponds to a phase function that we picked from [Gkioulekas et al. 2013]. In each row, the left image is rendered with the original parameters and used for creating the reference embedding (the blue points in Figure 9-ab). The middle image is generated with the altered parameters provided by our algorithm (Algorithm 1 in the paper). We use it for the higher-order embedding (the yellow points in Figure 9-a). The right image is created with the altered parameters satisfying only the order-1 similarity relation. The corresponding embedding (which collapses to a 1D line) is in Figure 9-b of the paper. The middle and right images share the same altered scattering coefficient σ_s^* and are rendered in similar time.

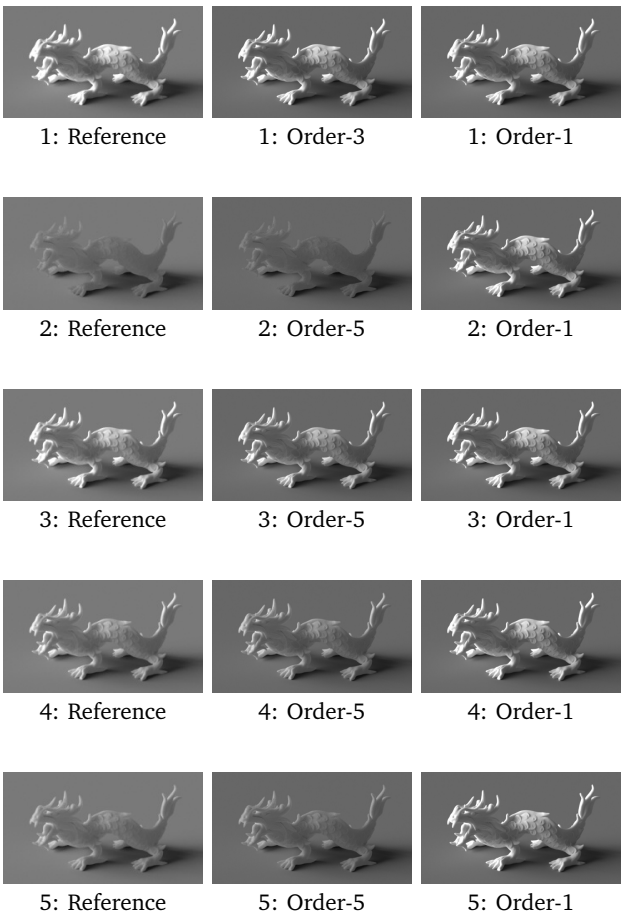

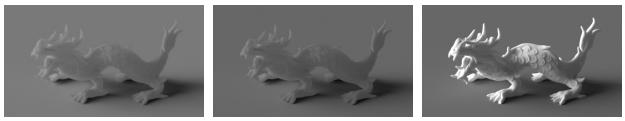

6: Reference | 6: Order-4 | 6: Order-1

7: Reference | 7: Order-3 | 7: Order-1

8: Reference | 8: Order-2 | 8: Order-1

9: Reference | 9: Order-3 | 9: Order-1

10: Reference | 10: Order-4 | 10: Order-1

11: Reference | 11: Order-3 | 11: Order-1

12: Reference | 12: Order-3 | 12: Order-1

13: Reference | 13: Order-2 | 13: Order-1

14: Reference | 14: Order-3 | 14: Order-1

15: Reference | 15: Order-2 | 15: Order-1

16: Reference | 16: Order-2 | 16: Order-1

17: Reference | 17: Order-2 | 17: Order-1

18: Reference | 18: Order-3 | 18: Order-1

19: Reference | 19: Order-3 | 19: Order-1

20: Reference | 20: Order-5 | 20: Order-1

21: Reference | 21: Order-5 | 21: Order-1

22: Reference | 22: Order-5 | 22: Order-1

23: Reference | 23: Order-5 | 23: Order-1

24: Reference | 24: Order-3 | 24: Order-1

25: Reference | 25: Order-5 | 25: Order-1

26: Reference 26: Order-4 26: Order-1

27: Reference 27: Order-4 27: Order-1

28: Reference 28: Order-5 28: Order-1

29: Reference 29: Order-5 29: Order-1

30: Reference 30: Order-4 30: Order-1

31: Reference 31: Order-4 31: Order-1

32: Reference 32: Order-4 32: Order-1

33: Reference 33: Order-4 33: Order-1

34: Reference 34: Order-4 34: Order-1

35: Reference 35: Order-1 35: Order-1

36: Reference 36: Order-2 36: Order-1

37: Reference 37: Order-4 37: Order-1

38: Reference 38: Order-3 38: Order-1

39: Reference 39: Order-4 39: Order-1

40: Reference 40: Order-4 40: Order-1

7.2 Phase Function Plots

This section contains the plots of all phase functions used to create the renderings in Section 7.1.

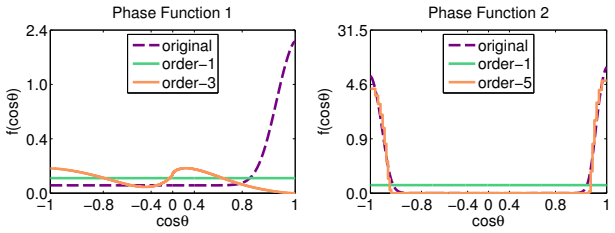

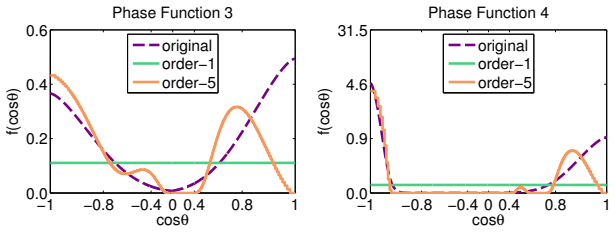

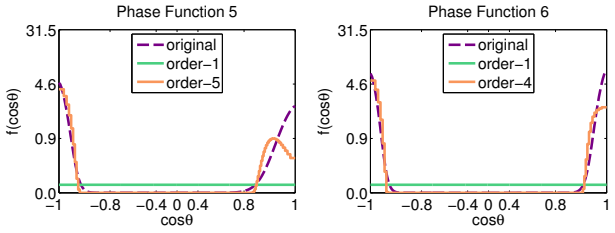

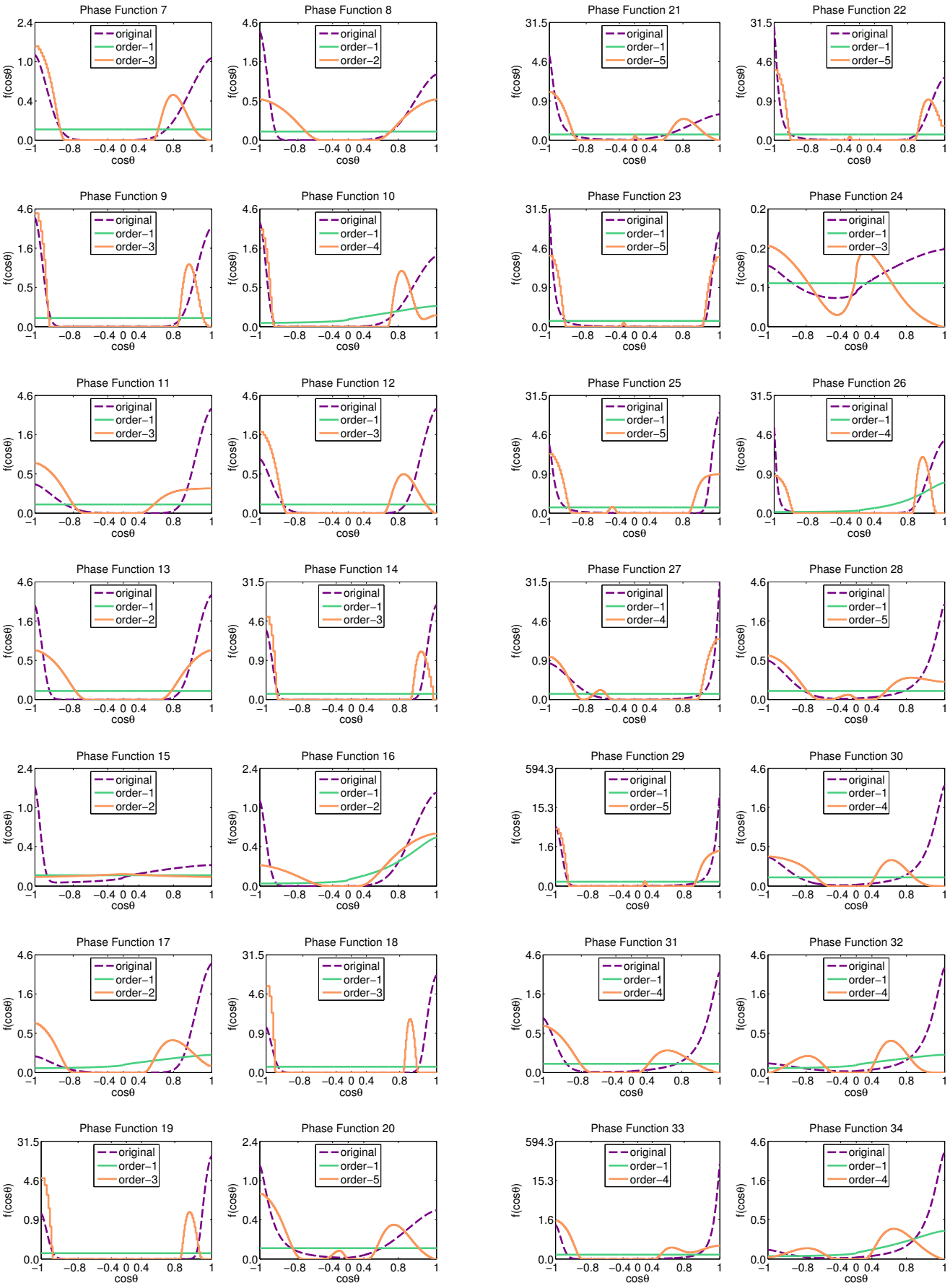
Phase Function 7
original
order−1
order−3
Phase Function 8
original
order−1
order−2
Phase Function 21
original
order−1
order−5
Phase Function 22
original
order−1
order−5
Phase Function 9
original
order−1
order−3
Phase Function 10
original
order−1
order−4
Phase Function 23
original
order−1
order−5
Phase Function 24
original
order−1
order−3
Phase Function 11
original
order−1
order−3
Phase Function 12
original
order−1
order−3
Phase Function 25
original
order−1
order−5
Phase Function 26
original
order−1
order−4
Phase Function 13
original
order−1
order−2
Phase Function 14
original
order−1
order−3
Phase Function 27
original
order−1
order−4
Phase Function 28
original
order−1
order−5
Phase Function 15
original
order−1
order−2
Phase Function 16
original
order−1
order−2
Phase Function 29
original
order−1
order−5
Phase Function 30
original
order−1
order−4
Phase Function 17
original
order−1
order−2
Phase Function 18
original
order−1
order−3
Phase Function 31
original
order−1
order−4
Phase Function 32
original
order−1
order−4
Phase Function 19
original
order−1
order−3
Phase Function 20
original
order−1
order−5
Phase Function 33
original
order−1
order−4
Phase Function 34
original
order−1
order−4
f(cosθ)
cosθ

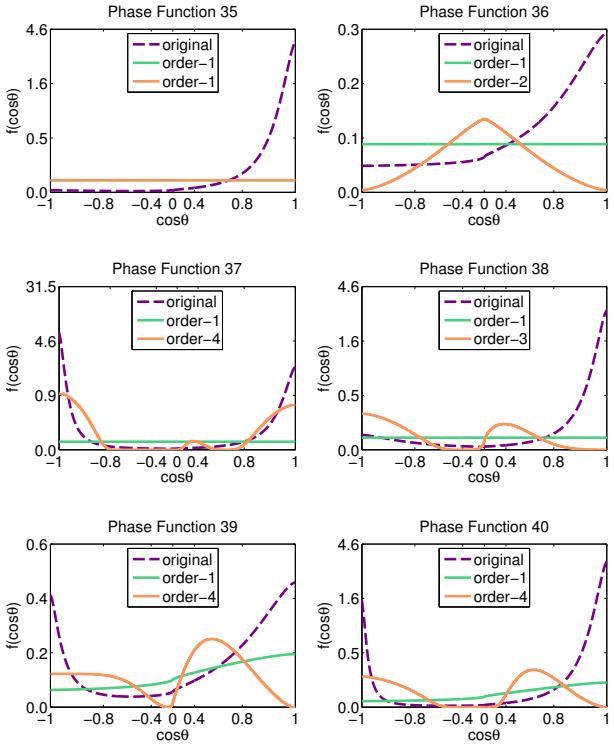

References

DEBEVEC, P. 1998. Rendering synthetic objects into real scenes: Bridging traditional and image-based graphics with global illumination and high dynamic range photography. In *Proceedings of SIGGRAPH 1998*, 189–198.

GKIOULEKAS, I., XIAO, B., ZHAO, S., ADELSON, E. H., ZICKLER, T., AND BALA, K. 2013. Understanding the role of phase function in translucent appearance. *ACM Trans. Graph. 32*, 5, 147:1–147:19.

VAN DEN EYNDE, G. 2005. *Neutron Transport with Anisotropic Scattering*. PhD thesis, Ph. D. Thesis, Université Libre de Bruxelles.

WYMAN, D. R., PATTERSON, M. S., AND WILSON, B. C. 1989. Similarity relations for anisotropic scattering in Monte Carlo simulations of deeply penetrating neutral particles. *Journal of Computational Physics 81*, 1, 137–150.

WYMAN, D. R., PATTERSON, M. S., AND WILSON, B. C. 1989. Similarity relations for the interaction parameters in radiation transport. *Applied optics 28*, 24, 5243–5249.